Single and multilayer metamaterials fabricated by nanoimprint lithography

Single and multilayer metamaterials fabricated by nanoimprint lithography

I Bergmair[1], **B Dastmalchi**[2], **M Bergmair**[2], **A Saeed**[2], **W Hilber**[3], **G Hesser**[2], **C Helgert**[4], **E Pshenay-Severin**[4], **T Pertsch**[4], **E B Kley**[4], **U Hübner**[5], **N H Shen**[6], **R Penciu**[7], **M Kafesaki**[7], **C M Soukoulis**[6,7], **K Hingerl**[2], **M Muehlberger**[1] and **R Schoeftner**[1]

[1] Functional Surfaces and Nanostructures, PROFACTOR GmbH, Im Stadtgut A2, 4407 Steyr-Gleink, Austria

[2] Center for Surface and Nanoanalytics, Johannes Kepler University Linz, Altenbergerstrasse 69, 4040 Linz, Austria

[3] Institute of Microelectronics and Microsensors, Johannes Kepler University Linz, Altenbergerstrasse 69, 4040 Linz, Austria

[4] Institute for Applied Physics, Friedrich-Schiller-Universität Jena, Max Wien Platz 1, 07743 Jena, Germany

[5] Institute of Photonic Technology, Albert-Einstein-Straße 9, 07743 Jena, Germany

[6] Ames Laboratory and Department of Physics and Astronomy, Iowa State University, Ames, IA 50011, USA

[7] Institute of Electronic Structure and Laser, Foundation for Research Technology Hellas (FORTH), University of Crete, 71110 Heraklion, Crete, Greece

E-mail: iris.bergmair@profactor.at

Abstract

We demonstrate for the first time a fast and easy nanoimprint lithography (NIL) based stacking process of negative index structures like fishnet and Swiss-cross metamaterials. The process takes a few seconds, is cheap and produces three-dimensional (3D) negative index materials (NIMs) on a large area which is suitable for mass production. It can be performed on all common substrates even on flexible plastic foils. This work is therefore an important step toward novel and breakthrough applications of NIMs such as cloaking devices, perfect lenses and magnification of objects using NIM prisms. The optical properties of the fabricated samples were measured by means of transmission and reflection spectroscopy. From the measured data we retrieved the effective refractive index which is shown to be negative for a wavelength around 1.8 μm for the fishnet metamaterial while the Swiss-cross metamaterial samples show a distinct resonance at wavelength around 1.4 μm.

(Some figures in this article are in colour only in the electronic version)

1. Introduction

Materials are called negative index materials (NIMs) when the designed structures provide resonances for the electric and magnetic field such that negative refraction occurs [1]. Those effects are mostly shown by various design approaches incorporating single functional layers of, for example, so-called fishnet [2] and Swiss-cross [3] patterns. Though the transition from such thin film to three-dimensional (3D)-like materials has been thoroughly investigated theoretically [4], only a few approaches have been reported to practically achieve 3D negative index materials, mainly by using e-beam lithography or focused ion beam patterning [5–8]. Those fabrication techniques are often restricted to small area footprints and/or consist of numerous and technologically complicated process steps.

On the other hand, truly 3D negative index materials promise to enable numerous novel and breakthrough applications such as perfect lenses [9] and magnification tools using negative index prisms [10]. Therefore it is of paramount importance to fabricate such structures with a
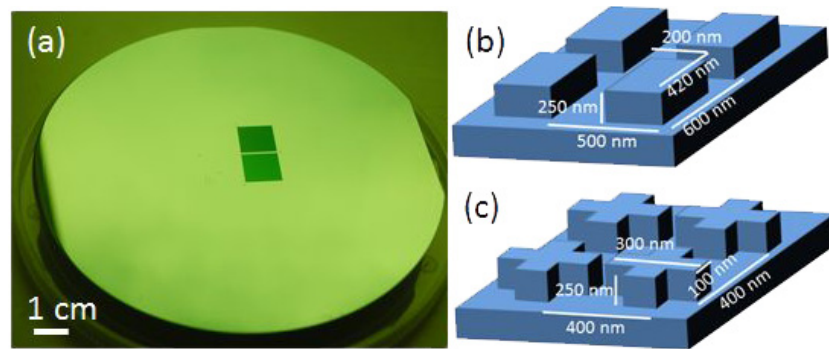
Figure 1. (a) Photograph of a silicon master containing fishnet and Swiss-cross stamp patterns. (b), (c) Schematics of the nanostructures containing all geometrical details. The fishnet has a period of 500 and 600 nm in *x*- and *y*-direction respectively, while the Swiss-cross has a lattice period of 400 nm in either lateral direction. The smallest feature size—the arm width of the crosses—is 100 nm.
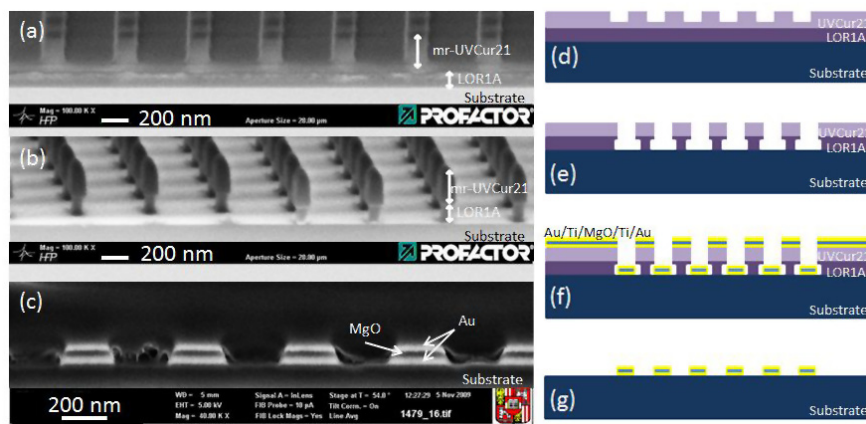
Figure 2. Cross-sectional SEM images (left) and schematic drawing of different process steps (right). (a), (d) Imprint into mr-UVCur21 on LOR1A layer. (b), (e) Imprint after etching and development to achieve recessed sidewalls. (f) Deposition of Au, Ti, MgO, Ti, Au. (c), (g) Final sample after lift-off.

fast and cost efficient technique on a large area suitable for industrial production. Nanoimprint lithography (NIL) is such a promising technology, since it allows us to fabricate large areas within a few seconds using a nanostructured stamp [11, 12]. So far, only a few approaches resulting in single layer NIMs using this method have been reported [13].

In this work we demonstrate the fabrication of single functional layers of NIM structures on silicon substrates using a two layer lift-off process. For the first time, we stack these layers to achieve a 3D NIM material. The single layers are peeled off from the substrate by using an ultraviolet (UV)-curable hybrid polymer as 'glue'. Repeating this process several times and stacking the single layers on top of each other leads to a 3D NIM. The stacking process can be performed on quartz, borofloat glass as well as on flexible substrates and takes only a few minutes. Our method inhibits an unlimited versatility with respect to the actual shape and composition of the nanostructures, therefore working for split ring resonators (SRRs) [14] as well as for double gold layer structures separated by a dielectric, as is the case for the fishnet and Swiss-cross patterns. Hence it is applicable to a very wide and general class of nanostructured thin films and optical metamaterials.

2. Experiments

We demonstrate the method using the examples of a fishnet [2] and a Swiss-cross pattern [3], being prototypical NIM structures whose optical functionality is well understood. In the present case, these NIMs were designed such that the characteristic optical resonances occur for the fishnet and for the Swiss-cross patterns at wavelengths of 1.8 μm and 1.4 μm, respectively. Based on these designs a NIL master on a 4″ silicon wafer which contains two areas of 0.9×0.9 cm^2 with protruding crosses and squares, respectively, was fabricated by means of e-beam lithography (figure 1). In the following, we will detail the established and optimized NIL process.

The master is treated with the anti-sticking layer BGL-GZ-83 from PROFACTOR GmbH [15] and replicated into a working stamp material [16] which is used for the imprint process. First a two layer resist system is spin coated. It consists of LOR1A from MicroChem as transfer layer and the UV-NIL resist mr-UVCur21 from Micro Resist Technology GmbH [17]. The working stamp is pressed into the mr-UVCur21 which fills up the nanostructures within the stamp. For the imprint process an EVG® 620 mask aligner and a compliant layer are used [18]. During contact of stamp and resist, the resist is UV-cured and after separation of stamp and
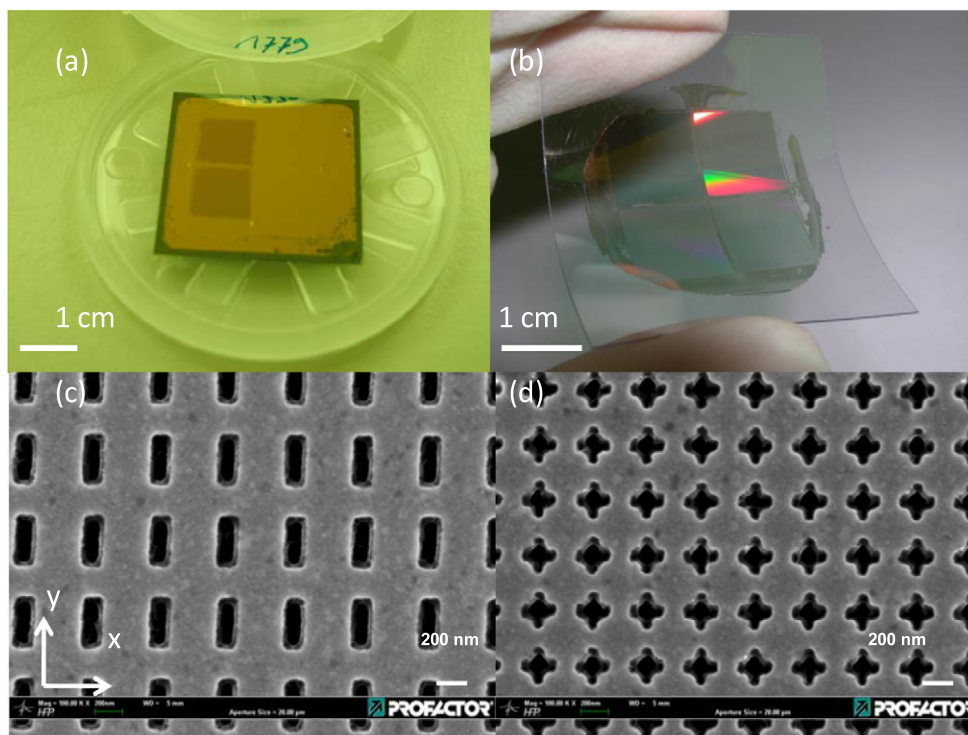
Figure 3. (a) Photograph of the single layer NIM sample and (b) transfer printed gold grating on a flexible foil. Top-view SEM images of (c) the single functional fishnet layer and (d) the Swiss-cross NIMs.

resist a negative copy of the structures on the substrate remains (figures 2(a) and (d)).

After etching through the residual resist layer and the LOR1A layer, the LOR1A is developed using diluted MF24A such that recessed sidewalls are achieved (figures 2(b) and (e)). They are necessary for a successful lift-off process of such small structures. For the fishnet and Swiss-cross structure a layer sequence of 30 nm Au, 2 nm Ti, 40 nm MgO, 2 nm Ti, 30 nm Au is deposited on the NIL patterned substrate (figure 2(f)). This layer sequence will be denoted as a functional layer of the NIM. The Ti is important to increase the adhesion of the Au to the MgO. Ti is omitted between the Au and the substrate to guarantee a successful transfer printing process. The lift-off has to be done carefully since the adhesion of the gold layer to the substrate is weak. Ultrasonic baths do not work and tend to lift off the whole patterned thin film. Therefore we use a technique which we call the 'whirlpool technique'. The sample is immersed in a remover and air bubbles are created on the sample surface by a water ray which is directed into the remover. These so-created air bubbles on the sample surface lift off the remnant resist such that clean nanostructures remain on the substrate (figures 2(c) and (g)). Figure 3 shows photographs and scanning electron microscope (SEM) images of a single layer NIM sample fabricated with this modified lift-off process. To achieve a potential 3D material we proceeded in stacking single functional layer samples (figure 3(a)).

As indicated in figure 4(a), the silicon substrate carrying the fabricated nanostructures is brought into contact with Ormocomp [17], which was diluted and spin cast on a borofloat glass substrate (figure 4(b)). The Ormocomp fills up the holes

in the fishnet structure and is cured with UV light through the glass substrate (figure 4(c)). This method is similar to a usual NIL process and therefore can be performed in the EVG® 620 mask aligner. When the two substrates are separated, the gold structures are peeled off from the silicon substrate and stuck to the glass substrate (figure 4(d)). Their preferred adhesion on Ormocomp on the glass substrate is due to the good adhesion of Ormocomp to gold. This process works on nearly all substrates including flexible foils (figure 3(b)). By repeating this transfer printing process one can build up several functional layers on top of each other (figures 4(e)–(g)). Figure 5 shows such stacked double and triple layer samples. The distance between the NIM layers is 100 nm but can be adjusted by changing the spin speed and/or dilution of the Ormocomp material. The whole transfer process takes only a few minutes and is therefore a fast, reproducible and powerful tool to build up 3D materials for industrial use. The achieved alignment accuracy for NIL fabricated samples is around 100 nm and below using Moiré patterns [19]. By means of complementary simulations which are omitted here for reasons of brevity, we verified that this alignment accuracy satisfies the design tolerances of the targeted NIMs. These simulations were done for a misalignment of five layers with a maximum 50 nm shift of each single layer in x- and y-directions. Apart from some modifications of the optical spectrum which are of minor relevance for the overall functionality, the targeted resonances remained nearly unaltered for all calculated cases. In addition, the resonance peaks were confirmed by our measurements of the stacked sample which had a potential misalignment of the order of 100 nm.
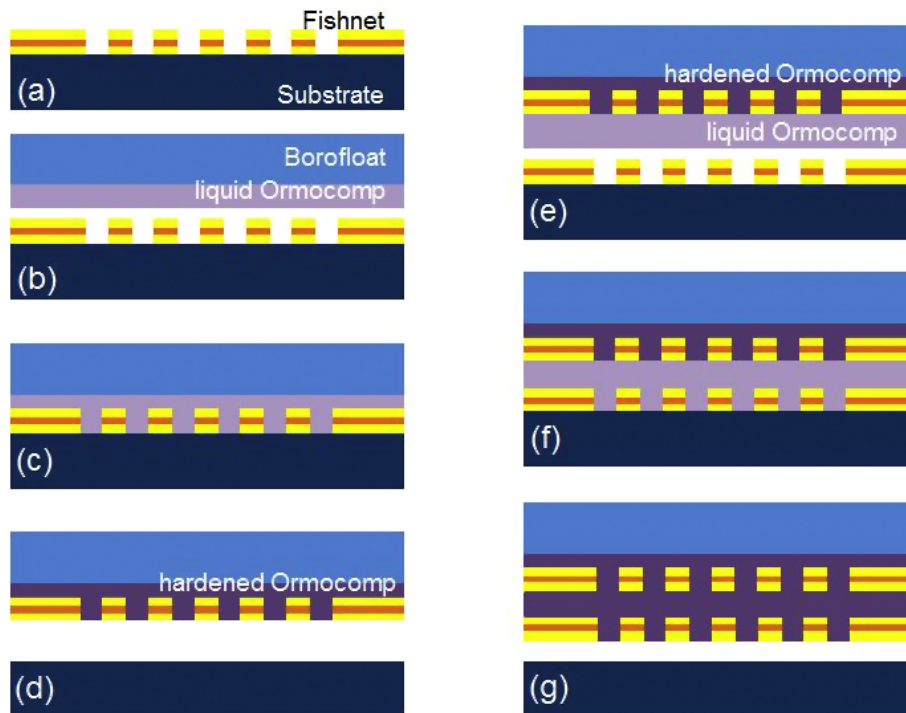
Figure 4. Schematic transfer printing process: (a) fabricated fishnet/Swiss-cross pattern, (b) spin coating of diluted Ormocomp on borofloat substrate or foil, (c) printing and hardening of Ormocomp with UV light, (d) peeling of a single layer NIM structure, (e) spin coating of diluted Ormocomp on a first transfer printed layer, (f) printing and hardening of Ormocomp with UV light, (g) peeling of the second layer NIM structure.
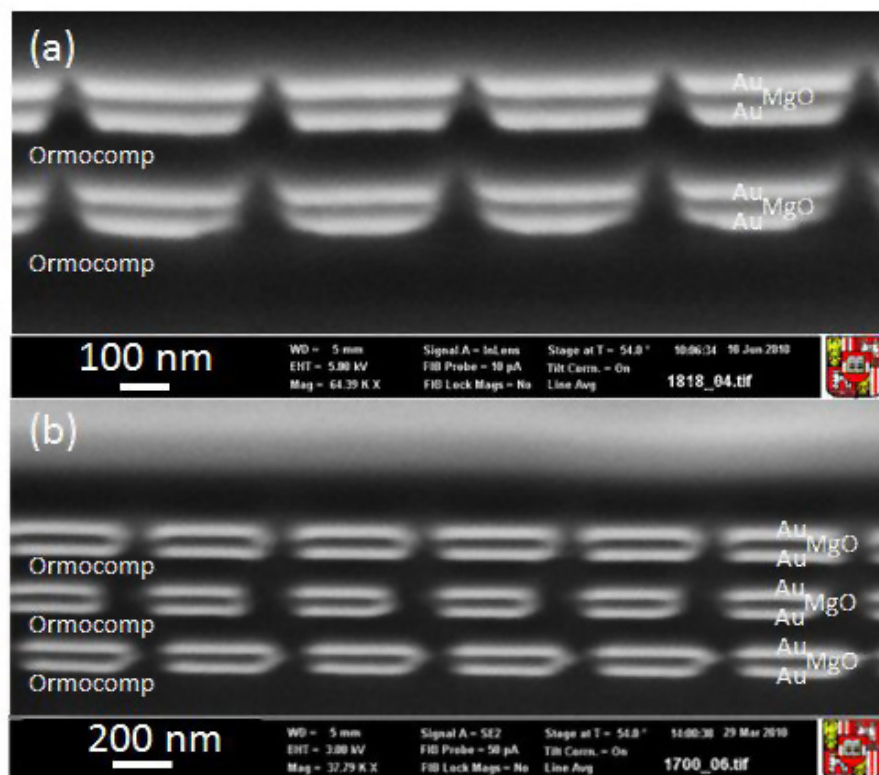
Figure 5. SEM cross-sectional images of a stacked NIM material. (a) Two layers of a Swiss-cross NIM and (b) three layers of a fishnet NIM with a vertical distance of 100 nm between the distinct functional layers. The structures are homogeneously embedded in Ormocomp.
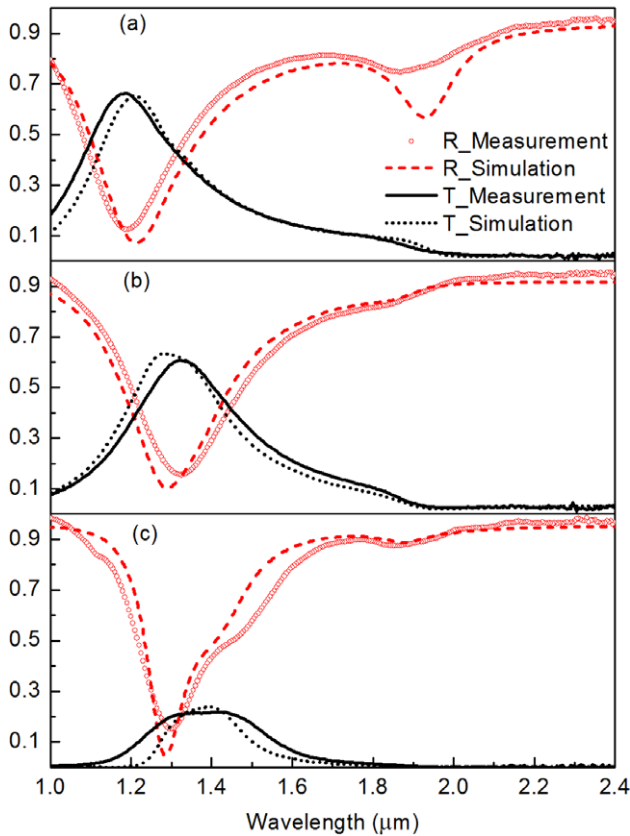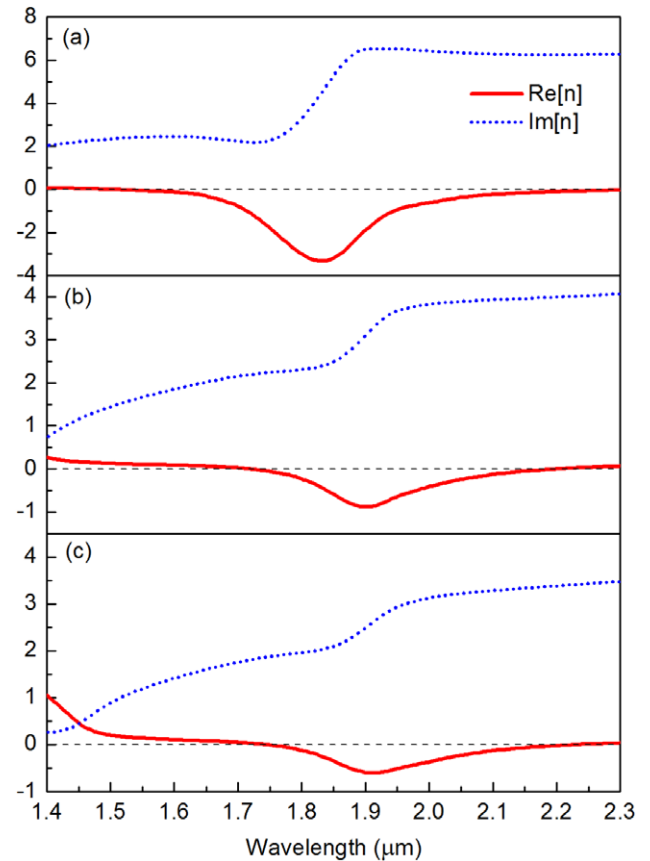
Figure 6. Measured transmission and reflection curves of (a) single layer fishnet, (b) transfer printed fishnet and (c) double layer fishnet metamaterials. The resonance associated with a negative refractive index occurs at a wavelength of around 1.8 μm.

Figure 7. Retrieved effective refractive index n of (a) single layer, (b) transfer printed single layer and (c) double layer fishnet metamaterial.

3. Optical characterization

The fabricated fishnet and Swiss-cross metamaterials were optically characterized by transmission and reflection spectroscopy for a wavelength range between 1 and 2.4 μm with the commercially available spectrometer Lambda 950 from Perkin Elmer. All transmission and reflection measurements were performed at a light incidence angle of 0° (transmission) or 6° (reflection) with respect to the substrate planes. The measurement data were normalized to the plane substrate without the NIM structures.

In figure 6 the reflection and transmission curves are shown for the fishnet single layer, transfer printed single layer and double layer fishnet for x-polarized light as depicted in figure 3(c). Assuming the homogenizability of NIMs, their spectral properties can be conveniently summarized in terms of effective material properties such as the magnetic permeability μ and the electric permittivity ε, or, as an additional quantity, the effective refractive index n. Making use of a well established retrieval algorithm [20], we can assign a negative n at wavelengths around 1.8 μm for the fishnet NIM (figure 7) and at 1.4 μm for the Swiss-cross sample for normally incident light. In passing, we note the restricted validity of the application of effective material properties such as μ and ε for nanoscale heterostructures [21], nevertheless they are still considered as a useful tool to gain preliminary insight into the physics of such materials. Further information

may be obtained by measuring the spectral response at different angles of light incidence, which is the subject of a forthcoming contribution due to the complexity of this issue [22, 23].

4. Discussion of results

The applicability of the utilized retrieval algorithm implicitly assumes a sufficient agreement between the measured and simulated data. For the case shown here, the simulated and measured optical response of the samples correspond quite closely, although the resonance peak obtained from the measurements is slightly weaker and broadened than predicted by rigorous coupled wave analysis (RCWA) at least for the single layer. This peak broadening is most likely correlated to sample imperfections such as small deviations of the hole widths all over the sample area. From visual inspection, we evaluate the percentage of defects on the surfaces of our samples to be below 1%, while the defect distribution is quite uniform. Nevertheless when measuring the optical response at different spots of the sample area, the transmission and reflection curves are virtually indistinguishable. We may therefore conclude that the optical response can be perfectly reproduced using our optimized NIL fabrication method. It shall be mentioned, however, that the actual agreement between measured and simulated data was always reported to be less than perfect in the current literature—regardless of the actual fabrication method, e.g. electron beam lithography or

focused ion beam milling. Furthermore we wish to mention that, according to our simulations and long-term observations, the material properties generally have a larger influence on the optical response than the unavoidable geometric deviations. Specifically, the grain size of the metal and humidity within the MgO may shift the resonance peak to larger wavelengths.

During the transfer printing the NIM layer is embedded in Ormocomp, which usually weakens and red-shifts the resonance peak. This is due to the fact that Ormocomp has a refractive index around 1.4, therefore higher than air. The overall transmission of multilayer NIMs further decreases with the number of subsequently stacked NIM layers. For instance, the three layer fishnet NIM shown in figure 5(b) features a transmission close to zero at the resonance peak around 1.8 μm and is therefore not included in figure 7. This fact shows that further optimization of the design is necessary, but this was beyond the scope of this work which focuses on the technological achievements. We suggest that the layer distances and geometric details of the NIM designs may be further tailored to reduce losses and to create samples with satisfying optical properties.

5. Conclusion

In this work we have shown the fabrication of single layer NIM structures using the examples of state-of-the-art fishnet and Swiss-cross metamaterials. Furthermore a fast, NIL based, highly reproducible stacking process for such layers to achieve 3D NIMs was developed. This achievement constitutes a long-term-aspired milestone toward the cost efficient fabrication of NIM materials in order to transfer them into an application-oriented environment. We assessed the optical response of the fabricated samples by means of optical spectroscopy and complementary numerical simulations, and verified a negative index behavior at a wavelength of around 1.8 μm for the fishnet and at 1.4 μm for the Swiss-cross NIM, respectively. Although further design optimization may be necessary, our herein established technological process enables the stacking of a virtually unlimited number of nanostructured thin films and hence paves the way for the creation of so far unprecedented, truly 3D optical metamaterials.

Acknowledgments

References

[1] Veselago V G 1968 The electrodynamic of substances with simultaneously negative values of μ and ε *Sov. Phys.—Usp.* **10** 509

[2] Zhang S, Fan W, Panoiu N C, Malloy K J, Osgood R M and Brueck S R J 2005 Experimental demonstration of near-infrared Negative-Index Materials' *Phys. Rev. Lett.* **95** 137404

[3] Helgert C, Menzel C, Rockstuhl C, Pshenay-Severin E, Kley E-B, Chipouline A, Tünnermann A, Lederer F and Pertsch T 2009 Metamaterial in the near infrared *Opt. Lett.* **34** 704

[4] Rockstuhl C, Paul T, Lederer F, Pertsch T, Zentgraf T, Meyrath T P and Giessen H 2008 Transition from thin-film to bulk properties of metamaterials *Phys. Rev.* B **77** 035126

[5] Valentine J, Zhang S, Zentgraf T, Ulin-Avila E, Genov D A, Bartal G and Zhang X 2008 Three-dimensional optical metamaterial with negative refractive index *Nature* **455** 376

[6] Yao J, Liu Z, Liu Y, Wang Y, Sun C, Bartal G, Stacy A M and Zhang X 2008 Optical negative refraction in bulk metamaterials of nanowires *Science* **321** 930

[7] Liu N, Guo H, Fu L, Kaiser S, Schweizer H and Giessen H 2008 Three-dimensional photonic metamaterials at optical frequencies *Nat. Mater.* **7** 31

[8] Di Falco A, Ploschner M and Krauss T F 2010 Flexible metamaterials at visible wavelengths *New J. Phys.* **12** 113006

[9] Schurig D, Mock J J, Justice B J, Cummer S A, Pendry J B, Starr A F and Smith D R 2006 Metamaterial electromagnetic cloak at microwave frequencies *Science* **314** 977

[10] Wu Q, Schonbrun E and Park W 2007 Image inversion and magnification by negative index prisms *J. Opt. Soc. Am.* A **24** A45

[11] Chou S Y, Krauss P R and Renstrom P J 1995 Imprint of sub-25 nm vias and trenches in polymer *Appl. Phys. Lett.* **67** 3114

[12] Chou S Y, Krauss P R and Renstrom P J 1996 Nanoimprint lithography *J. Vac. Sci. Technol.* B **14** 4129

[13] Wu W, Yu Z, Wang S-Y, Williams R S, Liu Y, Sun C, Zhang X, Kim E, Shen Y R and Fang N X 2007 Midinfrared metamaterials fabricated by nanoimprint lithography *Appl. Phys. Lett.* **90** 063107

[14] Bergmair I, Mühlberger M, Hingerl K, Pshenay-Severin E, Pertsch T, Kley E-B, Schmidt H and Schöftner R 2010 3D materials made of gold using nanoimprint lithography *Microelectron. Eng.* **87** 1008

[15] http://www.profactor.at/en/nano/ produkte-verfahren-lizenzierbares/bgl-gz-83.html

[16] Mühlberger M, Bergmair I, Klukowska A, Kolander A, Leichtfried H, Platzgummer E, Loeschner H, Ebm Ch, Grützner G and Schöftner R 2009 UV-NIL with working stamps made from Ormostamp *Microelectron. Eng.* **86** 691

[17] www.microresist.de

[18] Mühlberger M *et al* 2008 Equalising stamp and substrate deformations in solid parallel-plate UV-based nanoimprint lithography *Microelectron. Eng.* **85** 822

[19] Mühlberger M *et al* 2007 A Moiré method for high accuracy alignment in nanoimprint lithography *Microelectron. Eng.* **84** 925

[20] Smith D, Schulz S, Markos P and Soukoulis C M 2002 Determination of effective permittivity and permeability of metamaterials from reflection and transmission coefficients *Phys. Rev.* B **65** 195104

[21] Menzel C, Paul T, Rockstuhl C, Pertsch T, Tretyakov S and Lederer F 2010 Validity of effective material parameters for optical fishnet materials *Phys. Rev.* B **81** 035320

[22] Minovich A, Neshev D N, Powell D A, Shadrivov I V, Lapine M, McKerracher I, Hattori H T, Tan H H, Jagadish C and Kivshar Y S 2010 Tilted response of fishnet metamaterials at near-infrared optical wavelengths *Phys. Rev.* B **81** 115109

[23] Menzel C, Helgert C, Üpping J, Rockstuhl C, Kley E B, Wehrspohn R B, Pertsch T and Lederer F 2009 Angular resolved effective optical properties of a Swiss cross metamaterial *Appl. Phys. Lett.* **95** 131104